

Supplementary material for

Intraseasonal to interannual variability of zooplankton biomass and standing stock inferred from ADCP backscatter in the eastern Arabian Sea

R. K. Sahu^{1,2}, D. Shankar^{1,2,*}, P. Amol^{1,3}, S. G. Aparna^{1,2}, D. V. Desai^{1,2}

¹*CSIR National Institute of Oceanography, Dona Paula, Goa-403004, India.*

*Corresponding author (Email: shankar@nio.res.in)

²*Academy of Scientific and Innovative Research (AcSIR), Ghaziabad, 201002, Uttar Pradesh, India*

³*CSIR-NIO, Regional Centre, Vishakhapatnam, 530017, Andhra Pradesh, India*

1 The supplementary material begins with a detailed comparison with the biomass cli-
2 matology from Aparna et al. (2022, A22). This is followed by a section on time-series
3 analysis tools like wavelets and filters. Next, a quality control test is carried out for the
4 Kollam backscatter data during 2020, when unusually low biomass was observed. Finally,
5 additional supplementary figures are included.

6 **S1 Comparison with biomass and zooplankton stand- 7 ing stock (ZSS) climatology of A22**

8 This section compares the climatology of both biomass and Zooplankton Standing Stock
9 (ZSS) from our recent data with those presented in A22 across three overlapping locations:
10 Mumbai, Goa, and Kollam. Both datasets show similar variability in biomass, with peaks
11 associated with the seasonal cycle occurring during winter off Mumbai and summer off
12 Kollam (Fig. S1a1–c1, a2–c2). The ZSS, integrated from 24 m to 104 m, also exhibits a
13 consistent dip after the summer monsoon, with weaker variability off Kollam (Fig. S1c1,
14 c2). Despite these similarities, a few differences are evident.

15 Data from recent years indicate relatively weaker biomass compared to A22, a weak-
16 ening that extends throughout the water column. This results in the 215 mg m^{-3} biomass
17 contour (D215) being shallower at all three locations, most notably off Goa, where D215,
18 previously aligned with the 23°C isotherm (D23), now lies approximately 20–40 m shal-
19 lower during January to April. The overall ZSS also drops due to this biomass weakening,
20 and the timing of maximum or minimum ZSS values doesn't always coincide between the
21 two datasets; for example, the ZSS maximum off Mumbai extends from February in A22
22 to February–March in the recent data. Off Kollam, the updated ZSS remains almost
23 constant around 25 mg m^{-2} , except for a minimum from July to August, whereas A22
24 shows a gradual biomass drop from March until September followed by an increase. This
25 difference is reflected in a lower correlation between A22's ZSS and the current ZSS
26 climatology off Kollam (0.60) compared to Mumbai (0.94) and Goa (0.98).

27 Finally, in the present study, chlorophyll-a (Chl-a) peaks across all locations in Au-
28 gust, with a smaller peak off Mumbai and Goa, and off Kollam, the mismatch between
29 zooplankton and phytoplankton trends remains consistent with A22's findings (Fig. S1d1,
30 d2). Climatological values of chlorophyll-a and ZSS are summarized in Table S1.

31 S2 Time-series analysis methods

32 This section describes the time-series analysis tools employed in this study to analyze
33 the biomass data. These tools include wavelets (Torrence and Compo, 1998), wavelet
34 coherence (Maraun and Kurths, 2004), and filters (Duchon, 1979). We used the Python
35 package `pycwt` for wavelet and wavelet coherence analysis, and the Lanczos function from
36 Ferret for filtering. While commonly used in physical oceanography, such methods are
37 less frequently applied in zooplankton studies due to practical limitations in collecting
38 the extensive time series data required. Unlike traditional biomass data, which are ob-
39 tained from volumetric zooplankton samples collected from the sea, the biomass data
40 discussed here are derived from hourly ADCP backscatter data extending over 4–6 years.
41 This substantial dataset allows us to investigate zooplankton variability across different
42 timescales, specifically within seasonal and intraseasonal bands, through the application
43 of these tools.

44 S2.1 Wavelet analysis and wavelet coherence

45 Understanding Fourier analysis lays the groundwork for wavelet analysis. Fourier trans-
46 forms break down a time series into sine and cosine components. This generates a power
47 spectrum that identifies dominant periodicities, such as annual (360 days) and semi-
48 annual (180 days) cycles. However, because Fourier analysis assumes signals are constant
49 over time, it can hide changes in non-stationary signals (oscillations whose amplitudes
50 aren't steady), potentially misrepresenting their true strength and variabilities.

51 Wavelet analysis addresses this limitation and helps identify when oscillating signals
52 are strongest within a time series (Torrence and Compo, 1998). For instance, while a
53 Fourier analysis might reveal a dominant 30-day period in biomass data (meaning biomass
54 increases for 15 days and then decreases for 15 days), it won't tell us when these 30-day
55 oscillations actually occur. Wavelets, however, resolve this. For example, as shown in
56 Figure 6a, wavelet analysis reveals that 30-day oscillations in Okha's data are prominent
57 specifically during the summer monsoon, with color intensity indicating signal strength.

58 For our study, wavelet analysis is especially useful for detecting both continuous sig-
59 nals, like the annual cycle, and intermittent bursts, particularly within the intraseasonal
60 range. Two key elements guide our interpretation:

- 61 • Cone of Influence (CoI): This shaded area highlights regions where edge effects
62 distort the wavelet results. Since our observations are a finite-length signal, wavelets
63 near the beginning or end of the data lack information outside the observation
64 period and cannot adequately resolve the desired frequency or period near the edges.
65 This distortion is more pronounced for lower frequencies (longer periods) and less
66 so for higher frequencies (shorter periods), creating a cone shape on the plot. The
67 results within the shaded regions of CoI should be interpreted with caution.
- 68 • Statistical Significance Contours: These contours help us determine if a strong peak
69 in the wavelet plot represents a true feature of the underlying signal or just a random
70 fluctuation. To assess this, we use a simple red noise (AR(1) or Markov) model as
71 our null hypothesis, which assumes more power at lower frequencies. In our wavelet
72 figures, the black contour specifically marks the 95% confidence interval.

73 For example, in Fig. 6b, the annual signal off Mumbai is both significant and well-
74 contained within the CoI (unshaded region). The figure also reveals significant semi-
75 annual and intraseasonal features.

76 Wavelet coherence builds on this framework by measuring localized correlations be-
77 tween two time series across both time and frequency (Maraun and Kurths, 2004). Unlike
78 traditional correlation, it captures time-varying relationships by normalizing the cross-
79 wavelet spectrum, yielding coherence values from 0 to 1. While within-band comparisons
80 are to be interpreted with caution, cross-period comparisons may be biased, particularly
81 at higher periods, due to the normalization scheme (Maraun and Kurths, 2004). Filter-
82 ing techniques can mitigate this, enabling reliable variability assessments across distinct
83 bands.

84 S2.2 Filtering method

85 Filtering techniques are used to isolate variability within a specific frequency band by
86 reducing signals outside that range. For example, when the biomass is filtered using a 5–
87 90-day period band-pass filter, we essentially create a new time series that only contains
88 oscillations between 5 and 90 days. This new time series will precisely tell us when
89 the biomass has reached the maximum or minimum with this band. Frequency band
90 selection can be based on well-established periods in the region, like the annual cycle,
91 or on prominent periods revealed by wavelet analysis. In this study, our specific choice
92 of frequency bands is motivated by prior research on the West India Coastal Current
93 (WICC), which utilized ADCP data—the source of our backscatter data—at these very
94 locations (Amol et al., 2014; Chaudhuri et al., 2020, 2021).

95 We employed the Lanczos filter, a common choice for oceanographic studies (Duchon,
96 1979). This filter is effective because it minimizes spectral leakage from unwanted signals
97 while preserving the target signal. However, a known limitation of the Lanczos filter
98 is data loss at the beginning and end of the time series due to edge effects. Any filter
99 requires preceding and succeeding data to work with. Therefore, they cannot be fully
100 applied near the edges, as there is simply no data before the beginning and after the end
101 of a finite-length time series. The length of this data gap at the edges depends on the
102 length of the filter window; filtering at lower frequencies will generate more significant
103 data gaps compared to higher frequencies.

104 While wavelet analysis shows how variability evolves across all timescales, Lanczos
105 filtering allows us to reliably examine variations within selected frequency bands. This
106 enables direct comparisons across different frequencies and intuitively visualize when
107 the highs and lows occur within the band (Table S3, S4; Figs.S4, S9). In our filtered
108 biomass data, negative values represent decreases relative to the mean, while positive
109 values indicate increases. Fig. S2 shows the filtered data for the annual (300–400 days)
110 and intra-annual band (100–250 days) that highlight variabilities over a specific band for
111 the entire data set.

112 S3 Quality control tests for Kollam (2020)

113 During 2020, the ADCP backscatter and, consequently, biomass, were unusually low off
114 Kollam (Fig. 3f). This coincided with the retrieval and redeployment of the ADCPs,
115 operations typically conducted near the year’s end for servicing the mooring. While

the weakening of signal strength appears attributable to natural causes (a drop in zooplankton biomass), it could also indicate potential data quality issues associated with the instrument itself. It's important to note that the same ADCP was used for data collection both before and after servicing.

A quick visual inspection shows that data before and after the servicing of moorings in October 2019 exhibit no significant differences in biomass (Fig. S10, top panel). However, following the December 2020 redeployment, there's a sudden increase in backscatter along with a blurring of the diurnal cycle. These abrupt increases in biomass, coupled with a drop in diurnal variability, are common occurrences. There are few instances of such increase in biomass, for example, between 30 m and 60 m during 27–29 September 2019 (Fig. S11), and at \sim 104 m during 27–29 September 2019 (Fig. S12).

To investigate this further, we compared in-situ biomass from volumetric zooplankton samples collected using a multi-plankton net (MPN) with corresponding ADCP backscatter values (Fig. S10, bottom panel). Since in-situ samples were only collected before retrieval and after deployment of the moorings, we have four MPN casts containing 16 data points at different depth ranges for comparison. Both datasets indicate that biomass generally decreases with depth, except in the 75–100 m range. This increase is evident in the depth-time plot (Fig. S10, top panel) as patches between 75 m and 125 m. These patches occur only during the night and appear to be part of the diurnal cycle. Barring three data points, all other data lie within one standard deviation of the least-squares fit between biomass and backscatter (Fig. S10, bottom panel). Two of these three outlying data points are from the 2019 post-deployment data.

Furthermore, backscatter data from Kanyakumari, located south and north of Kollam respectively, also show a drop in backscatter strength during 2020, though not as pronounced as off Kollam (Fig. 3).

These analyses strengthen the case for a real reduction in biomass rather than an instrumental error. The results underscore the importance of in-situ sampling in validating long-term ADCP-derived observations. Without these direct measurements, confidence in a year-long deployment would be limited. In this instance, low backscatter coincides with genuinely low biomass, demonstrating the complementary value of both approaches.

¹⁴⁶ References

- ¹⁴⁷ P. Amol, D. Shankar, V. Fernando, A. Mukherjee, S. G. Aparna, R. Fernandes, G. S.
¹⁴⁸ Michael, S. T. Khalap, N. P. Satelkar, Y. Agarvadekar, M. G. Gaonkar, A. P. Tari,
¹⁴⁹ A. Kankonkar, and S.P. Vernekar. Observed intraseasonal and seasonal variability of
¹⁵⁰ the West India Coastal Current on the continental slope. *J. Earth Syst. Sci.*, 123(5):
¹⁵¹ 1045–1074, 2014. [10.1007/s12040-014-0449-5](https://doi.org/10.1007/s12040-014-0449-5).
- ¹⁵² S. G. Aparna, D. V Desai, D Shankar, A. C Anil, Shrikant Dora, and R. R. Khedekar.
¹⁵³ Seasonal cycle of zooplankton standing stock inferred from ADCP backscatter mea-
¹⁵⁴ surements in the eastern Arabian Sea. *Prog. Oceanogr.*, 203:102766, 2022. [10.1016/j.pocean.2022.102766](https://doi.org/10.1016/j.pocean.2022.102766).
- ¹⁵⁵
- ¹⁵⁶ Anya Chaudhuri, D. Shankar, S. G. Aparna, P. Amol, V. Fernando, A. Kankonkar, G. S.
¹⁵⁷ Michael, N. P. Satelkar, S. T. Khalap, A. P. Tari, M. G. Gaonkar, S. Ghatkar, and R. R.
¹⁵⁸ Khedekar. Observed variability of the West India Coastal Current on the continental
¹⁵⁹ slope from 2009–2018. *J. Earth Syst. Sci.*, 129(1):57, 2020. [10.1007/s12040-019-1322-3](https://doi.org/10.1007/s12040-019-1322-3).
- ¹⁶⁰
- ¹⁶¹ Anya Chaudhuri, P Amol, D Shankar, S Mukhopadhyay, S. G Aparna, V Fernando,
¹⁶² and A Kankonkar. Observed variability of the West India Coastal Current on the
¹⁶³ continental shelf from 2010–2017. *J. Earth Syst. Sci.*, 130:1–21, 2021. doi: [10.1007/s12040-021-01603-4](https://doi.org/10.1007/s12040-021-01603-4).
- ¹⁶⁴
- ¹⁶⁵ Claude E Duchon. Lanczos filtering in one and two dimensions. *J. Appl. Meteorol.*
¹⁶⁶ *Climatol.*, 18(8):1016–1022, 1979. [10.1175/1520-0450\(1979\)018<1016:LFIOAT>2.0.CO;2](https://doi.org/10.1175/1520-0450(1979)018<1016:LFIOAT>2.0.CO;2).
- ¹⁶⁷
- ¹⁶⁸ Douglas Maraun and Jürgen Kurths. Cross wavelet analysis: significance testing and
¹⁶⁹ pitfalls. *Nonlin. Processes Geophys.*, 11(4):505–514, 2004. [10.5194/npg-11-505-2004](https://doi.org/10.5194/npg-11-505-2004).
- ¹⁷⁰
- ¹⁷¹ Christopher Torrence and Gilbert P Compo. A practical guide to wavelet analysis. *Bull.*
¹⁷² *Am. Meteorol. Soc.*, 79(1):61–78, 1998. [10.1175/1520-0477\(1998\)079<0061:APGTWA>2.0.CO;2](https://doi.org/10.1175/1520-0477(1998)079<0061:APGTWA>2.0.CO;2).

Table S1:

The climatological mean, standard deviation (SD), and range for satellite-derived chl-*a* (mg m^{-3}) and ZSS (g m^{-2}) computed at seven mooring locations. The climatology was calculated using available data from 2017 to 2023. The ZSS was determined by vertically integrating the climatological ADCP backscatter-derived biomass over the 24–140 m depth range. The table indicates an increase in ZSS range from south to north despite chl-*a* decreasing in the same direction.

Mooring location	Chlorophyll			ZSS		
	Mean	SD	Range	Mean	SD	Range
Okha	0.53	0.22	0.7	20.5	1.8	5.8
Mumbai	0.32	0.11	0.29	23.6	2.6	8
Jaigarh	0.28	0.08	0.26	24.2	2.9	9
Goa	0.25	0.08	0.24	21.2	1.9	6.3
Udupi	0.51	0.45	1.2	21.9	1.9	5.8
Kollam	0.58	0.67	2.32	24.6	1.1	4.1
Kanyakumari	0.53	0.47	1.58	20.1	0.6	2.4

Table S2:

The mean and SD of zooplankton biomass (mg m^{-3}) at 40 m and 104 m from daily re-gridded data across seven mooring locations. The last column presents the vertical range, calculated as the difference in mean biomass between 40 m and 104 m. Note that the SD at 104 m is lower than that at 40 m, except for Jaigarh.

Mooring location	40 m biomass		104 m biomass		Vertical Range (40 m - 104 m)
	Mean	SD	Mean	SD	
Okha	212.8	27.5	143.6	29.7	69.2
Mumbai	248.6	37.2	169.8	34.6	78.8
Jaigarh	253.5	38.2	170.4	50	83.1
Goa	216.3	35	153.5	37.2	62.8
Udupi	227.6	39.7	158.8	38.4	68.8
Kollam	247.9	55.5	184.2	48.3	63.7
Kanyakumari	192.3	34.4	157.5	23.8	34.8

Table S3:

SD of band-pass filtered biomass (mg m^{-3}) at 40 m and 104 m across seven mooring locations. Values for 104 m are shown in brackets. The biomass time-series were filtered for seasonal (100–400 days), annual (300–400 days), intra-annual (100–250 days), and intraseasonal (5–90 days) bands. The table shows that the intraseasonal variability (5–90 days) is often comparable to, and occasionally greater than, seasonal variability, suggesting pronounced fluctuations within season.

Mooring location	Seasonal (100–400 days)	Annual (300–400 days)	Intra-annual (100–250 days)	Intraseasonal (5–90 days)
Okha	6.3 (14.2)	2.3 (2.5)	4.9 (10.1)	17.7 (16.7)
Mumbai	19.1 (19.4)	5.6 (5.8)	13.2 (12.7)	20.2 (19.8)
Jaigarh	14.4 (20.9)	5.4 (7.9)	12.1 (12)	21.1 (23.8)
Goa	16.2 (17.8)	2.9 (6.5)	12.3 (10.1)	20.2 (17)
Udupi	22.1 (25)	4.9 (8.3)	15.2 (15.1)	23.7 (15.5)
Kollam	24.3 (15.6)	6.5 (5.1)	18.4 (10.9)	26.7 (17.4)
Kanyakumari	14.1 (9)	3.8 (3.4)	10 (5.6)	21.2 (14.3)

Table S4:

SD of band-pass filtered ZSS (g m^{-3}) and satellite chl-*a* (mg m^{-3}) across seven mooring locations. Values for chl-*a* are shown in brackets. Both time-series were filtered for seasonal (100–400 days), annual (300–400 days), intra-annual (100–250 days), and intraseasonal (5–90 days) bands. The ZSS is integrated over 24–120 m depth range provided valid biomass data is present in this depth range.

Mooring location	Seasonal (100–400 days)	Annual (300–400 days)	Intra-annual (100–250 days)	Intraseasonal (5–90 days)
Okha	0.7 (0.3)	0.2 (0.05)	0.5 (0.23)	1.1 (0.43)
Mumbai	1.6 (0.14)	0.5 (0.02)	0.9 (0.1)	1.2 (0.15)
Jaigarh	1.9 (0.16)	0.7 (0.02)	0.9 (0.12)	1.4 (0.22)
Goa	1.5 (0.08)	0.4 (0.02)	1 (0.06)	1.1 (0.14)
Udupi	1.8 (0.48)	0.3 (0.14)	1.3 (0.34)	1.2 (0.68)
Kollam	1 (0.57)	0.1 (0.16)	0.9 (0.45)	1.5 (0.7)
Kanyakumari	0.7 (0.5)	0.2 (0.1)	0.5 (0.3)	1.3 (0.7)

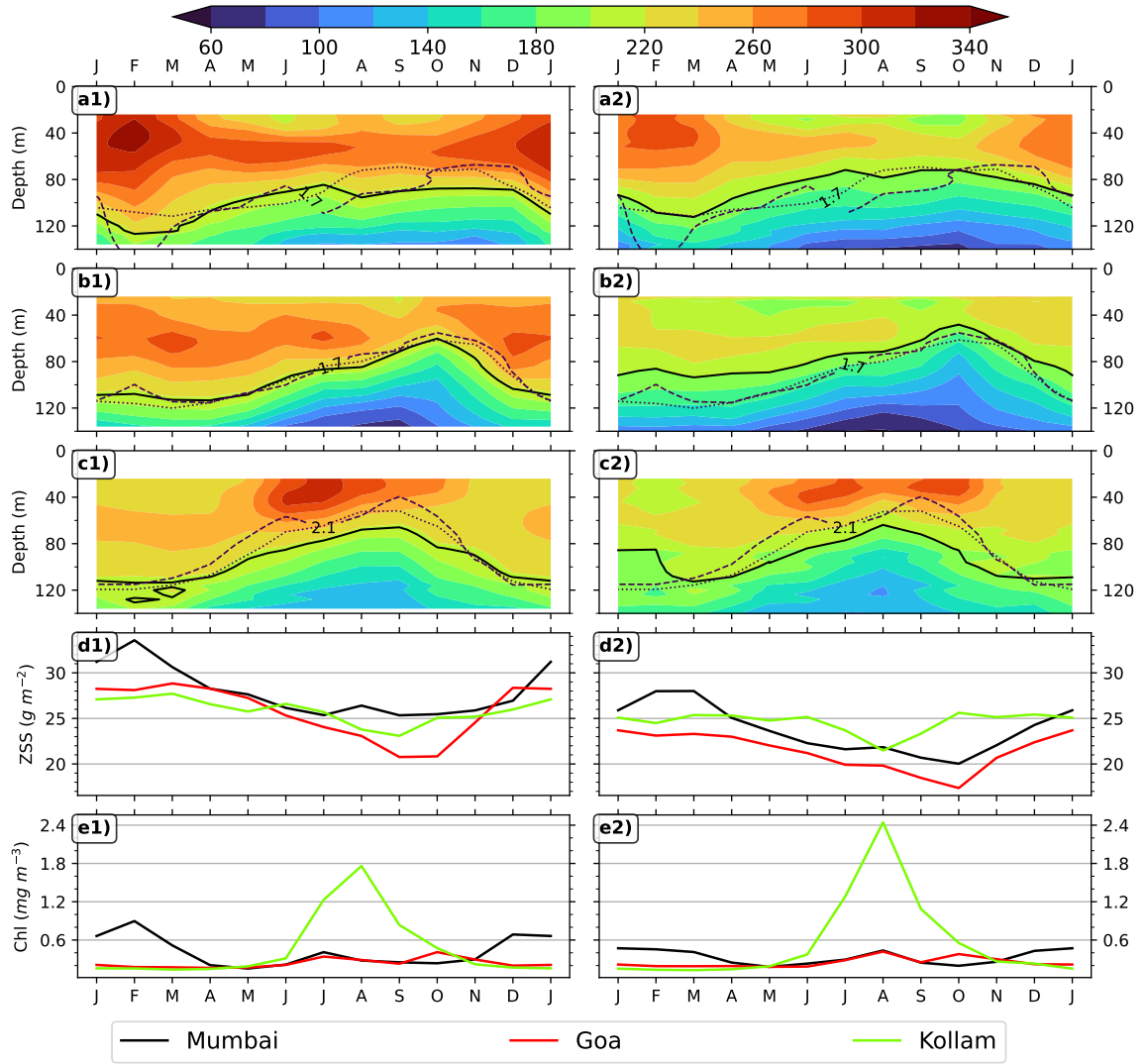


Figure S1: Comparison of monthly climatologies from the present dataset (right panel) with those from Aparna et al. (2022, A22) dataset (left panel). The present dataset spans 2017–2023, while A22’s climatology covered 2012–2020. The top panels display the monthly zooplankton biomass climatology for (a1, a2) Mumbai, (b1, b2) Goa, and (c1, c2) Kollam. The solid black line represents the 215 mg m^{-3} contour (D215), the dotted line indicates the 23°C isotherm depth, and dashed lines show oxygen contours. Panels d1 and d2 illustrate ZSS climatology (integrated over 24–140 m), while e1 and e2 show chl-*a* climatology. Note that A22 used SeaWiFS data for chl-*a*, whereas the present study uses L4 chl-*a* data from E. U. Copernicus Marine Service Information. Although recent lower biomass off Goa introduces a bias relative to the A22 climatology, the overall climatological patterns remain consistent between the two periods.

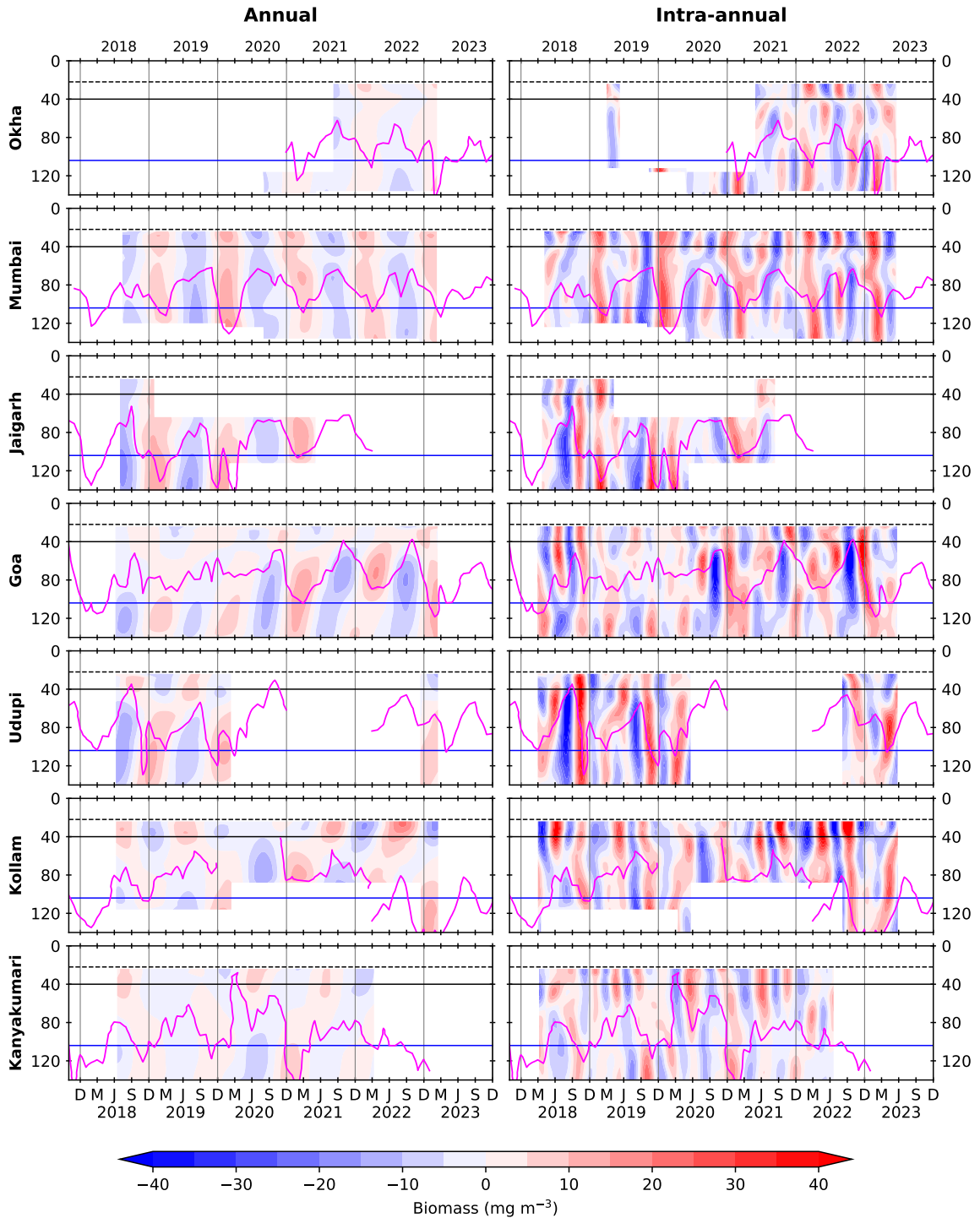


Figure S2: Biomass variability (mg m^{-3}) extracted using a band-pass filter for all locations. The left panel depicts the annual cycle (300–400 days) and the right panel shows the intra-annual variability (100–250 days). Horizontal solid black line and solid blue line represent 40 m and 104 m depths, respectively. The vertical black line separate the years. The dashed black line at 22 m marks the upper edge of the first bin (24 m), and the solid magenta curves denote *D*215 (or *D*175 off Okha and Kanyakumari), derived from the monthly biomass time series. The figure demonstrates that the intra-annual variability is stronger than the annual cycle at all locations.

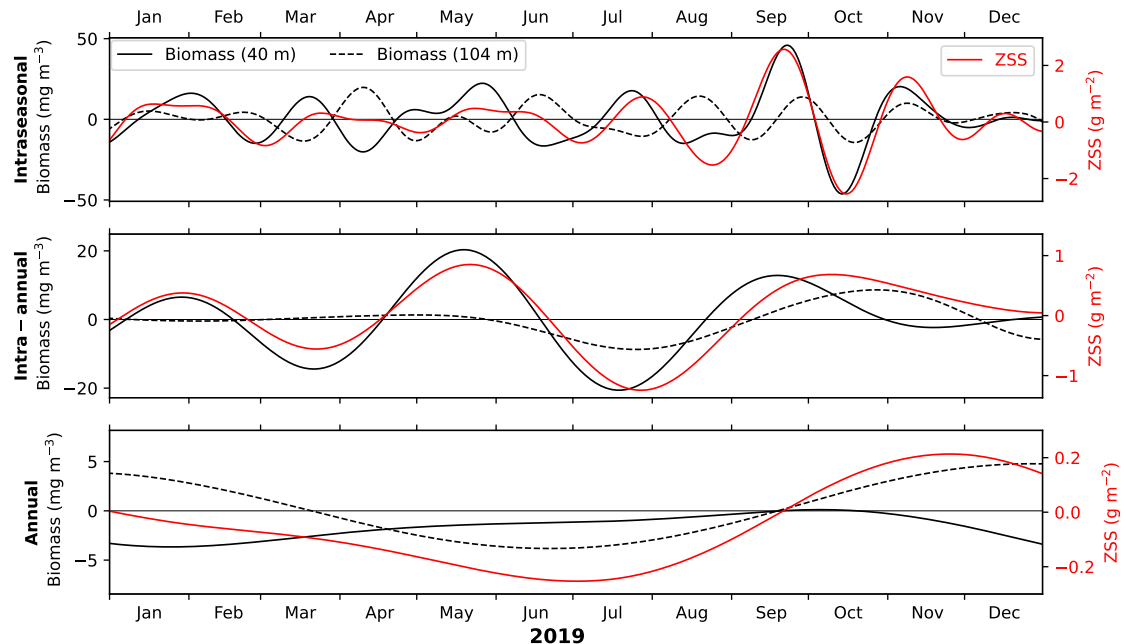


Figure S3: The figure compares band-passed filtered biomass (mg m^{-3}) at 40 m and 104 m with ZSS (g m^{-2}), integrated over 24–120 m, from Kanyakumari during 2019. Biomass at 40 m is shown as a black solid line, at 104 m as a black dashed line, while ZSS is a red solid line. The top panel illustrates intraseasonal biomass (30–90 days), the middle panel shows intra-annual biomass (100–250 days), and the bottom panel displays the annual biomass cycle (300–400 days). The comparison shows that the biomass at 104 m is frequently out of phase with upper-ocean biomass at 40 m across all three time scales. This phase difference between surface and subsurface biomass can either enhance or reduce the overall ZSS.

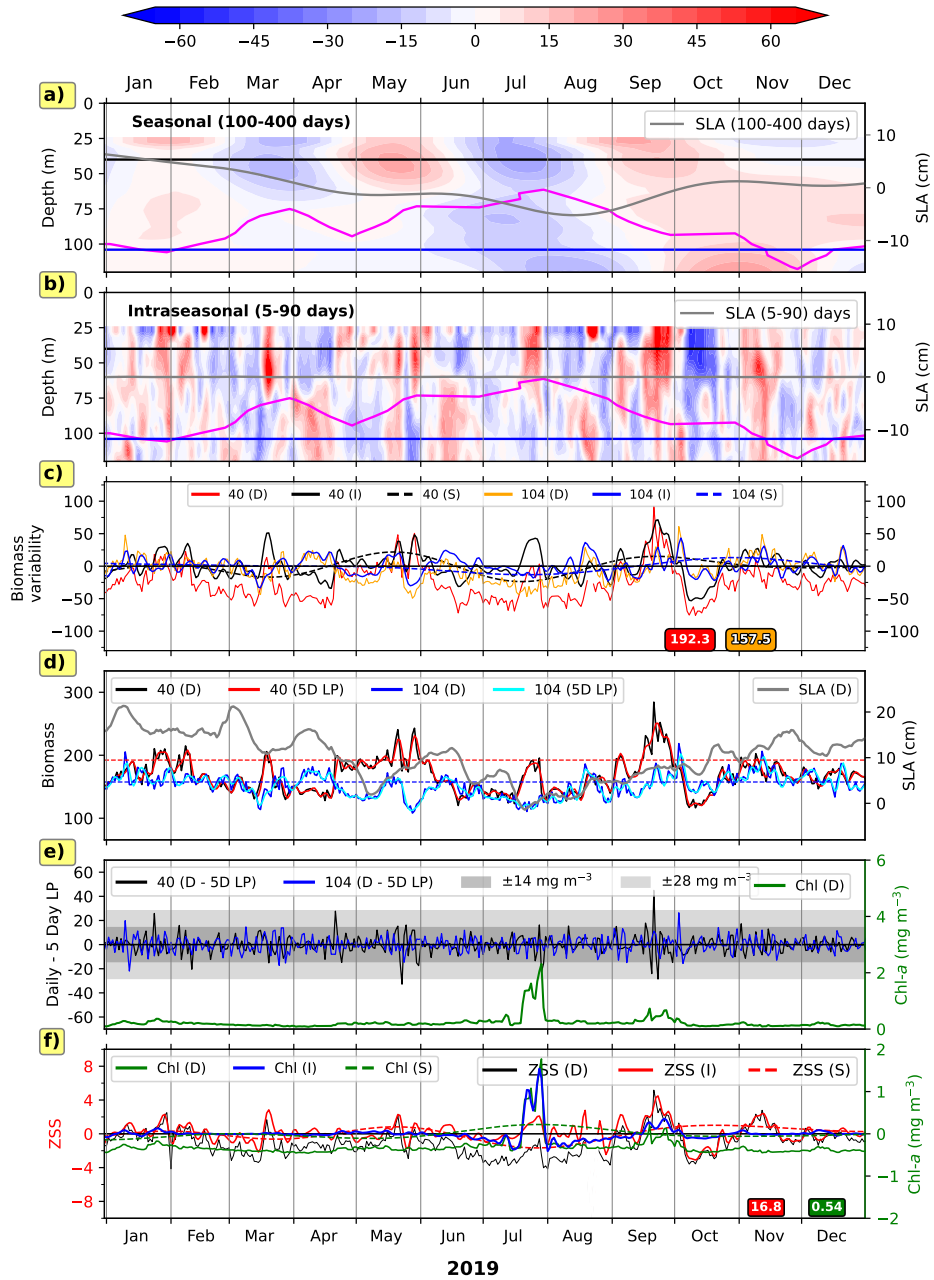


Figure S4: The figure shows a comparison of biomass variability (mg m^{-3}) in the seasonal (100–400 days) and intraseasonal (5–90 days) bands off Kanyakumari for the year 2019. For all panels, vertical grey lines separate the months. Panels (a) and (b) present time-depth plots of seasonal and intraseasonal biomass, respectively. Overlaid grey contours represent the corresponding sea level anomaly (SLA). Biomass at 40 m and 104 m depths is marked by black and blue horizontal lines. The magenta curves denote D175. Panel (c) shows the daily, intraseasonal, and seasonal biomass at 40 m and 104 m. The mean of the daily biomass time series for 40 m (red) and 104 m (orange) is indicated in the bottom right corner of this panel. Panel (d) compares daily SLA (grey) with daily and 5-day low-pass filtered biomass at 40 m and 104 m. Panel (e) illustrates the difference between daily and 5-day low-pass filtered biomass at both depths. Grey and light grey shaded regions denote the ± 1 SD and ± 2 SD bounds, respectively, derived from the backscatter-biomass relationship. Daily chl- a (green) is overlaid onto this panel. The bottom panel (f) shows daily satellite chl- a and ZSS, and their variability in the intraseasonal and seasonal bands.

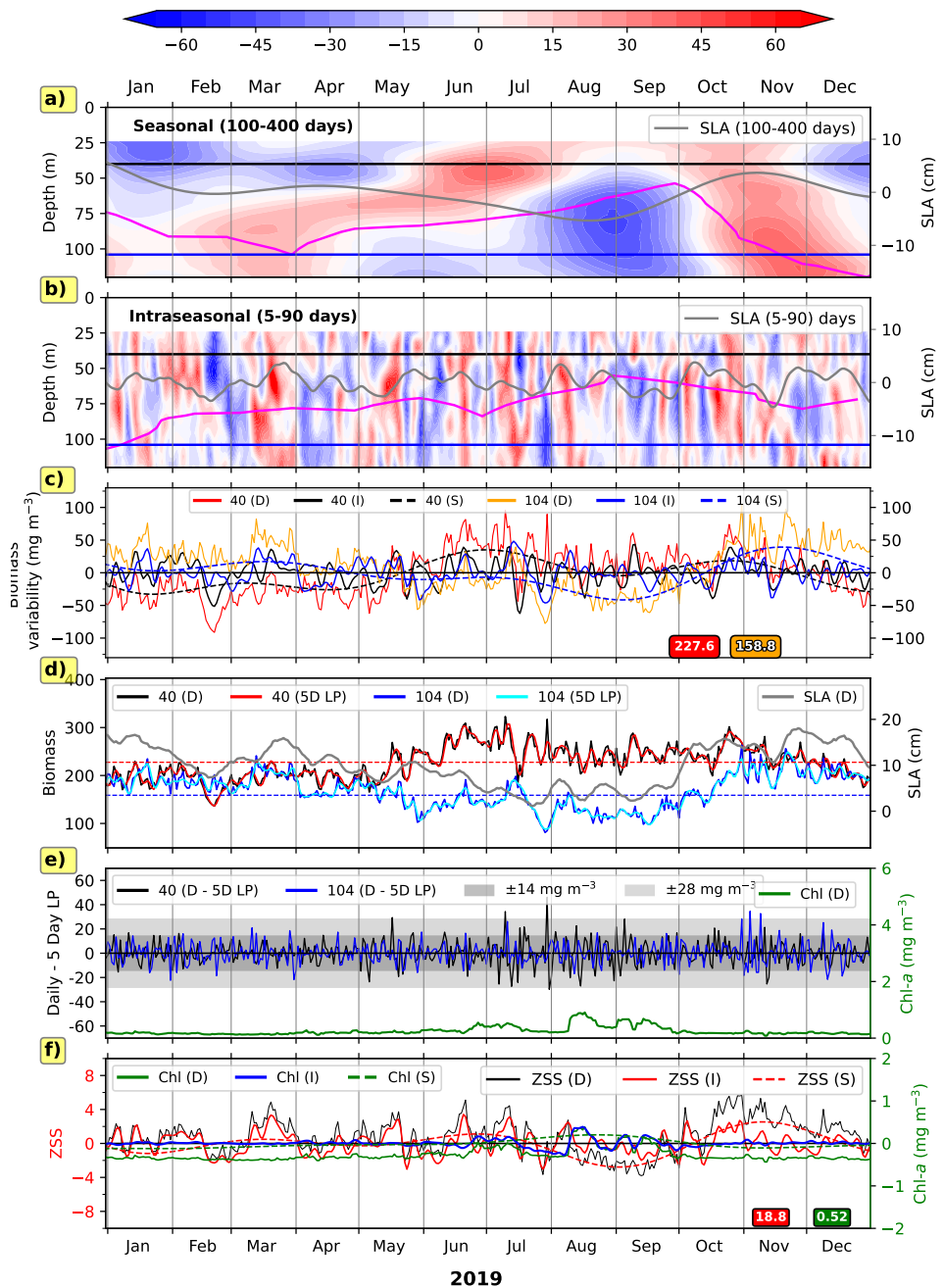


Figure S5: Same as in Fig. S4 but for Udupi with *D*215 curve in top two panels.

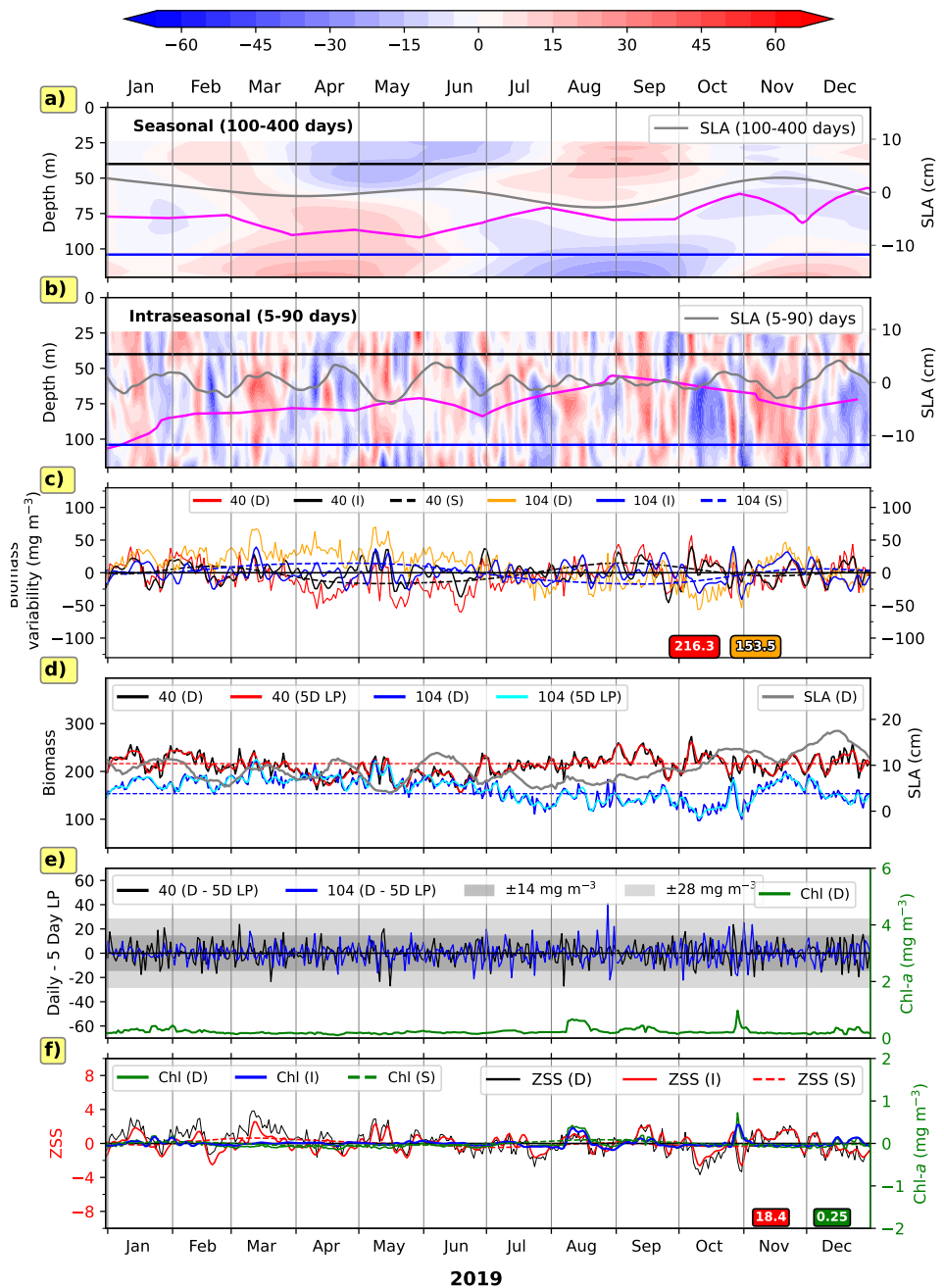


Figure S6: Same as in Fig. S4 but for Goa with *D*215 curve in top two panels.

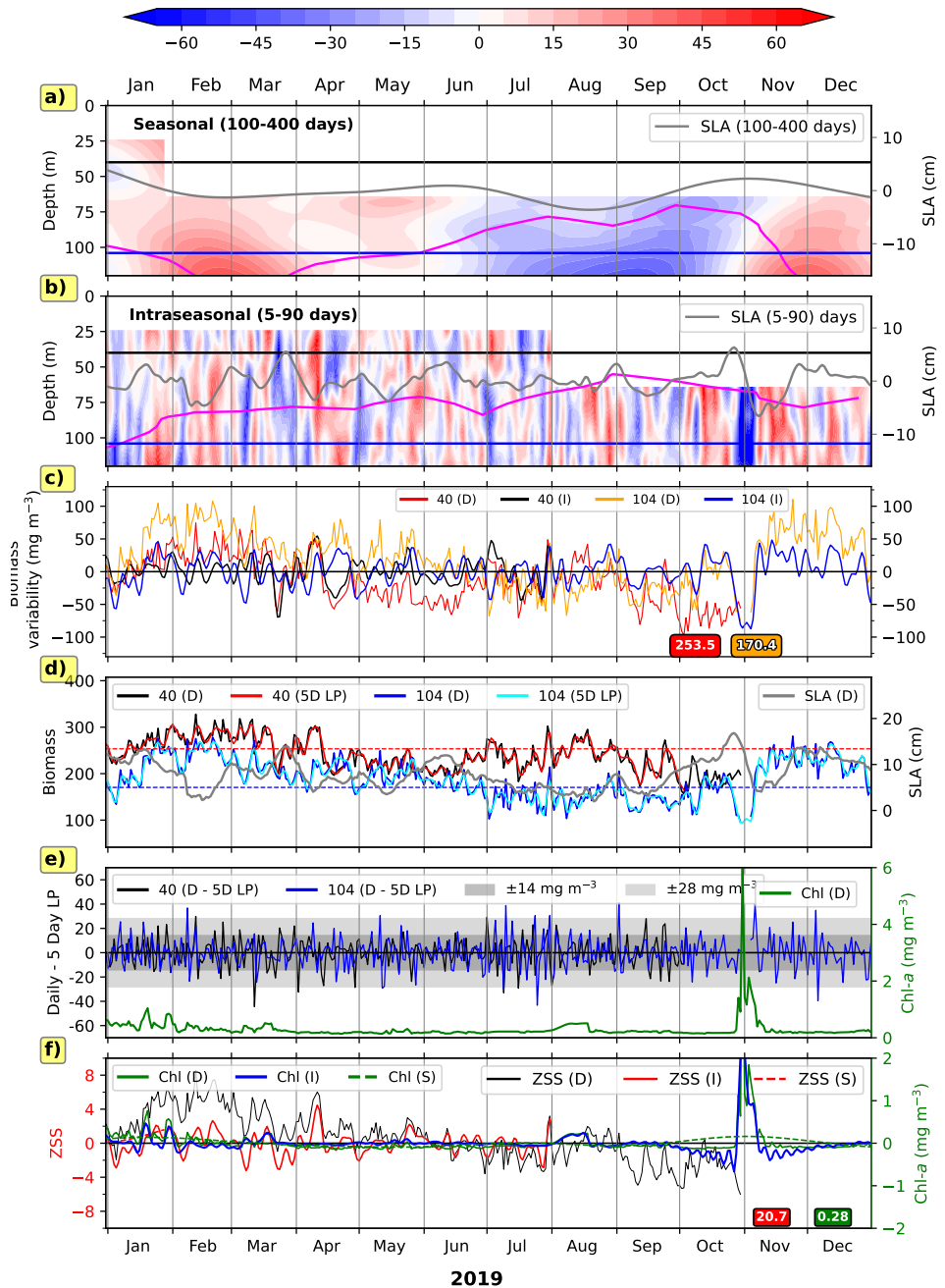


Figure S7: Same as in Fig. S4 but for Jaigarh with *D*215 curve in top two panels.

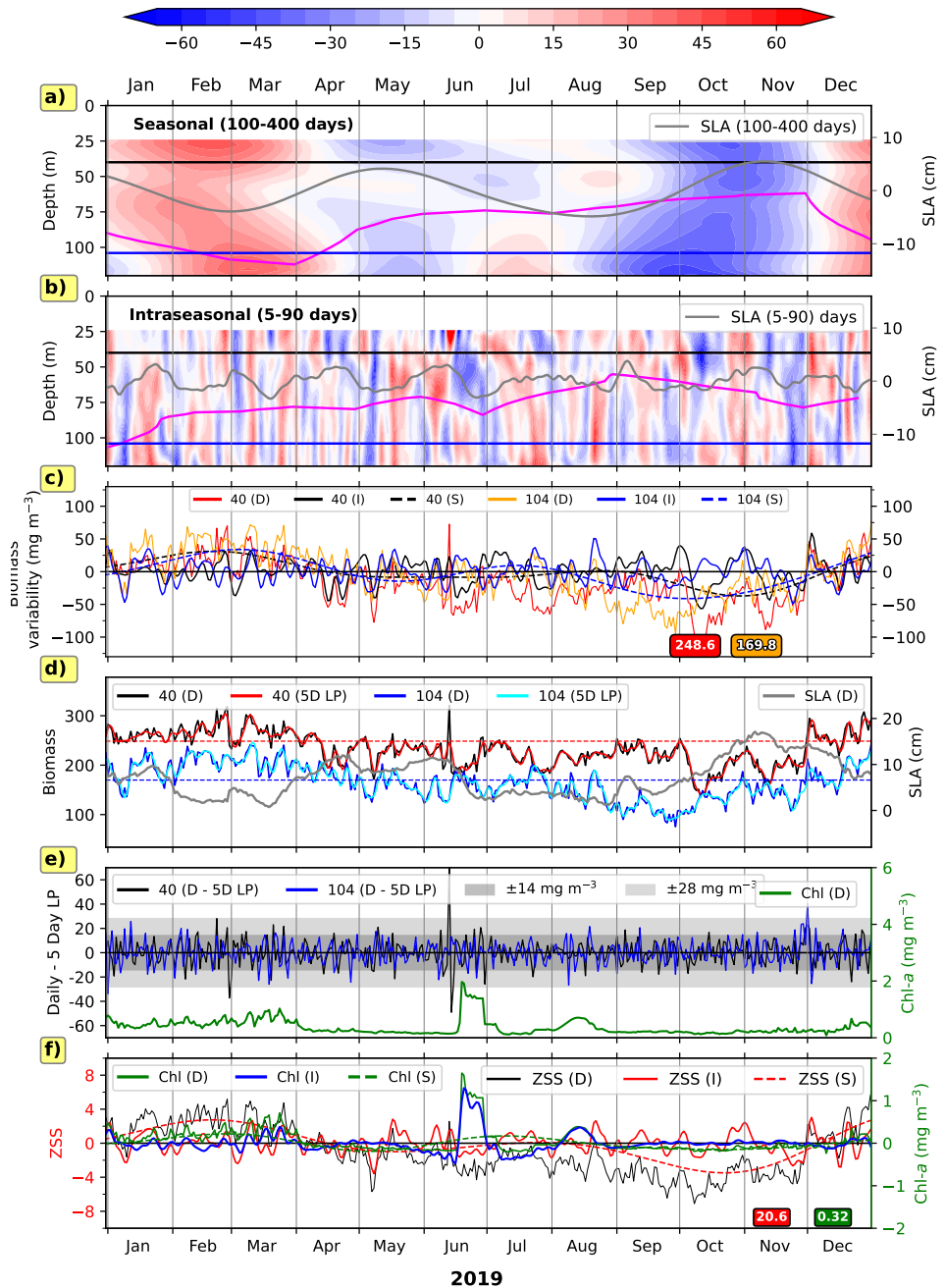


Figure S8: Same as in Fig. S4 but for Mumbai with D215 curve in top two panels.

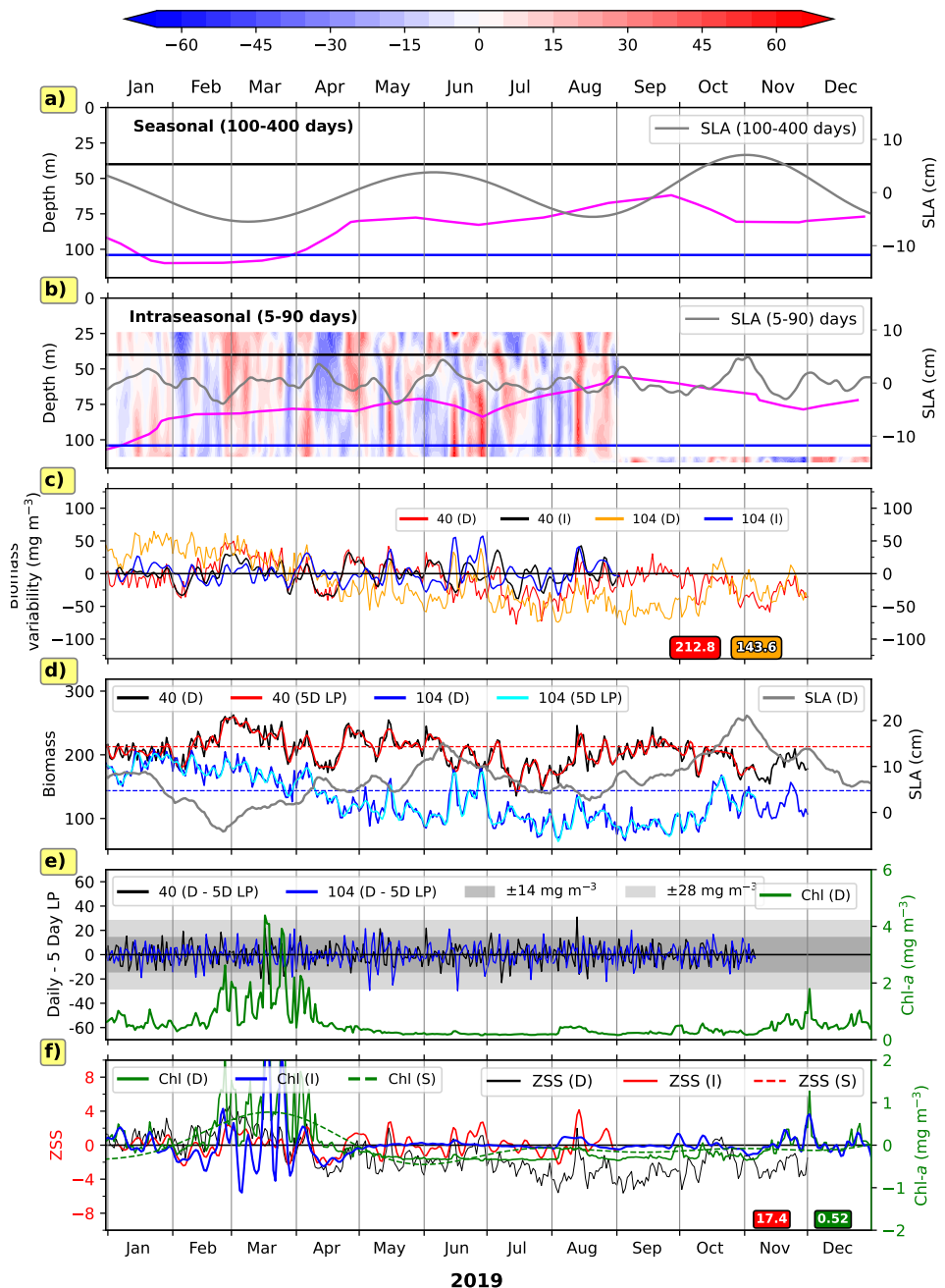


Figure S9: Same as in Fig. S4 but for Okha with D_{175} curve in top two panels.

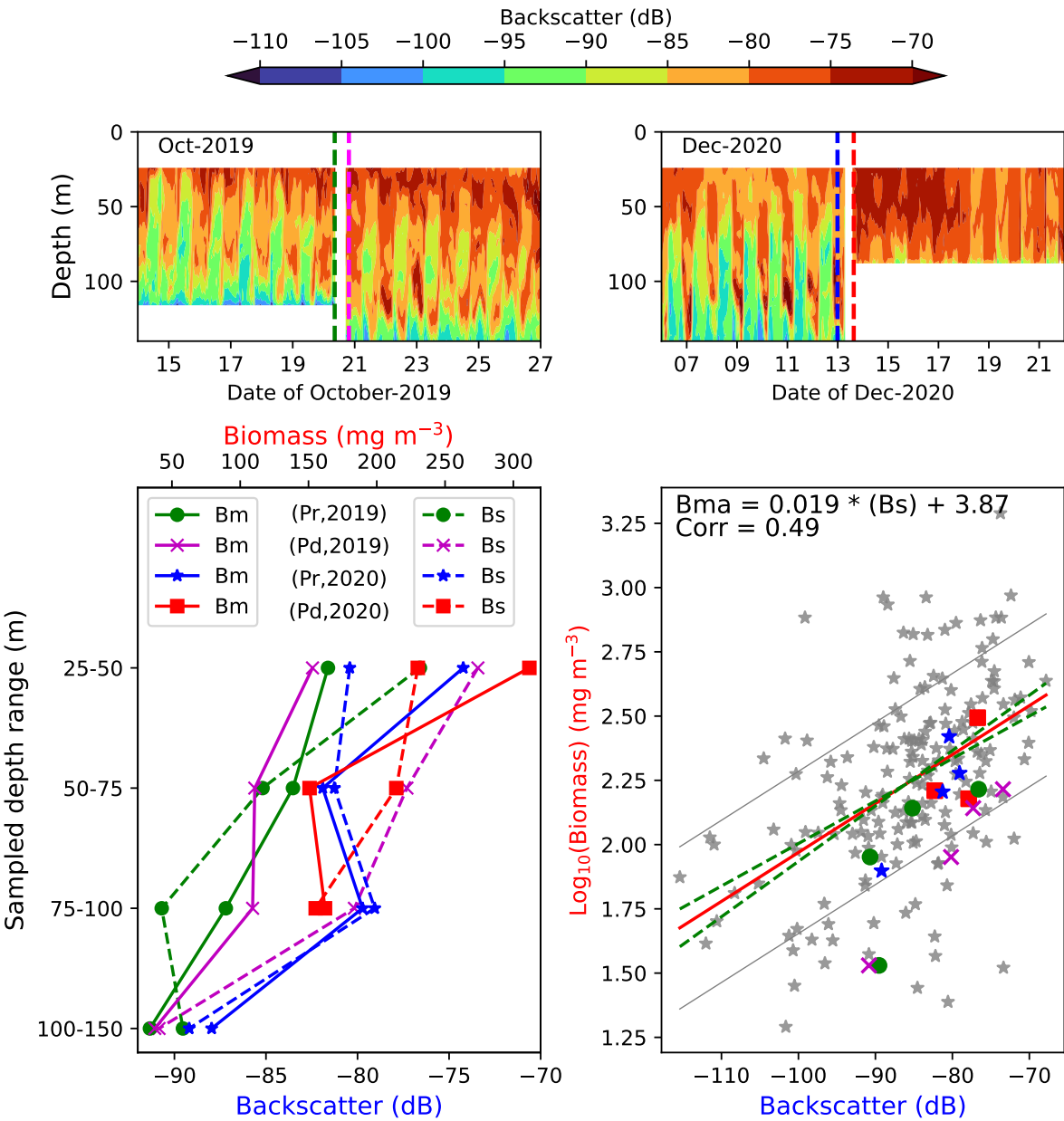


Figure S10: The figure presents Kollam ADCP backscatter (Bs) and its relationship with biomass data (mg m^{-3}) obtained from volumetric zooplankton samples collected during 2019 and 2020. The top panels display ADCP backscatter data before retrieval and after deployment. Specifically, the top-left (top-right) panel shows biomass data for October 2019 (December 2020), with retrieval and redeployment times marked by dashed green (blue) and dashed purple (red) vertical lines, respectively. The bottom-left panel shows biomass profiles (Bm) from zooplankton samples (solid lines), collected over selected sampling depth ranges, and corresponding ADCP backscatter profiles, integrated over the same depth ranges (dashed lines). These profiles are shown for the pre-retrieval (Pr) and post-deployment (Pd) phases of both 2019 and 2020. The bottom-right panel displays biomass (\log_{10} scale) plotted against backscatter from 2017 to 2023 for data from all seven stations. The ADCP backscatter derived biomass (Bma) is obtained using a linear regression line fitted between zooplankton biomass and ADCP backscatter. Data for Kollam in 2019 and 2020 are highlighted, with symbols and colors in this panel corresponding to those in the bottom-left panel.

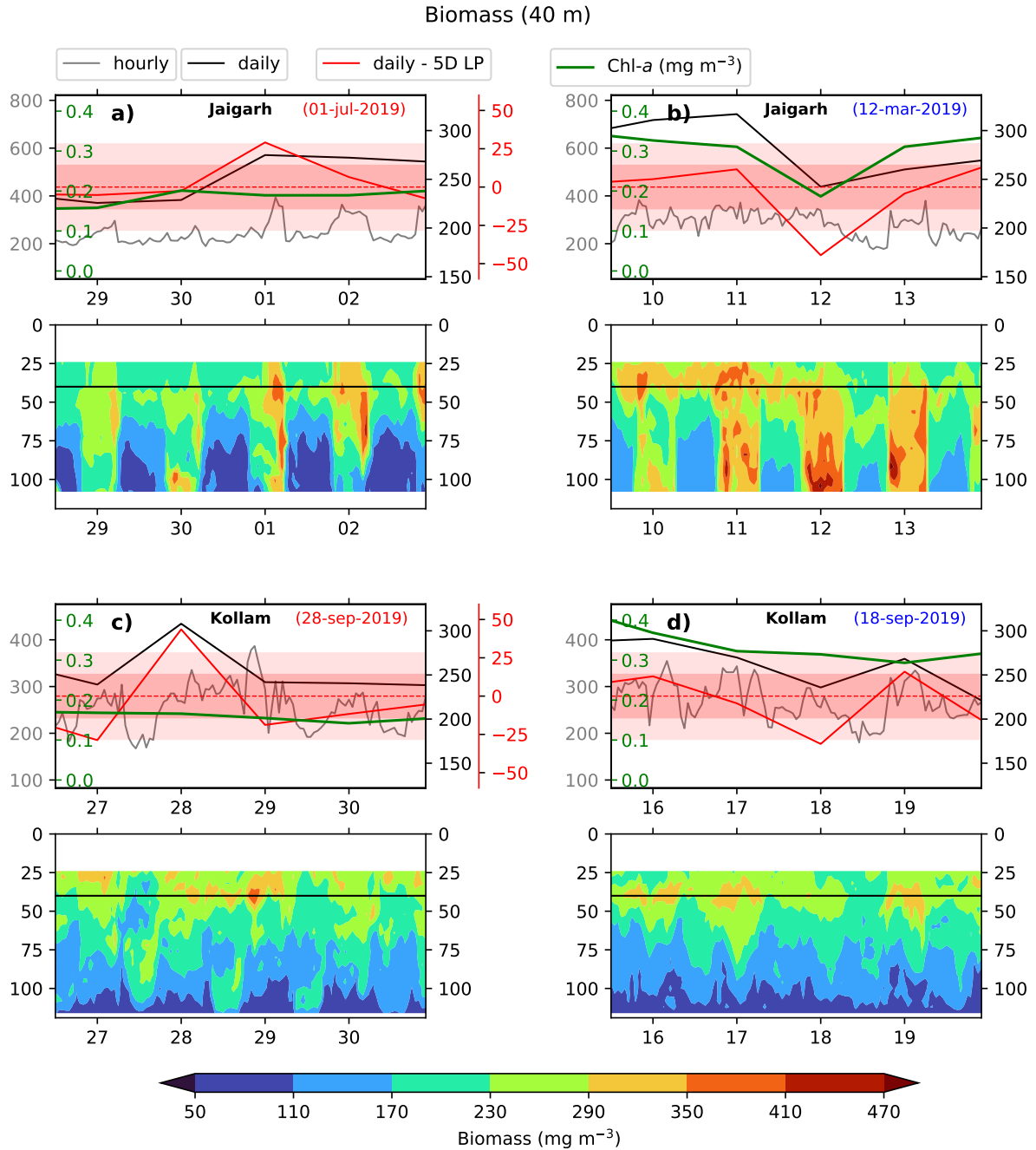


Figure S11: The figure illustrates biomass spikes and associated variability using daily time series and filtered data. Panels (a) and (b) show spikes as the difference between the mean-removed daily biomass time series (red) and the 5-day low-pass filtered biomass (black) at 40 m depth, off Jaigarh. Satellite chl- a is overlaid for the same duration. Note that the ordinates are different for each time series. Shaded regions represent ± 1 SD ($\pm 14 \text{ mg m}^{-3}$, red) and ± 2 SD ($\pm 28 \text{ mg m}^{-3}$, light red) from the mean-removed daily time series. The date of each spike event is noted in the top-right corner of each panel, with red and blue text indicating positive and negative spikes, respectively. The panels in the second row show depth-time plots for hourly biomass data; the black horizontal line marks the depth from which the time series for the top panels are extracted. Similarly, panels (c) and (d) show a positive and a negative spike event off Kollam. The bottom panels show the corresponding depth-time plots for biomass data.

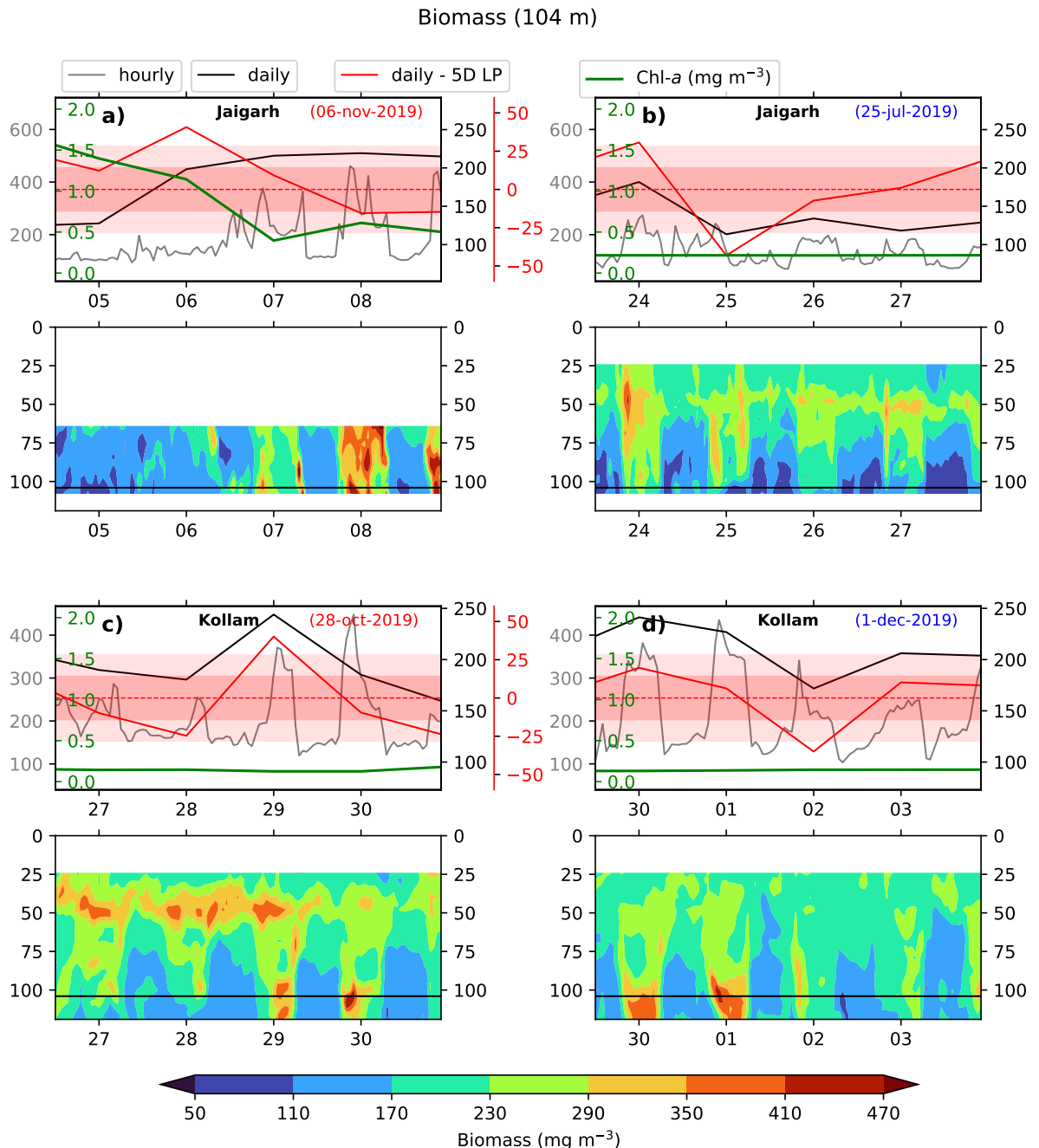


Figure S12: Same as Fig. S11 but for biomass at 104 m depth.